Survey of the wheat mycobiome associated with leaf blotch and head blight diseases in Sweden

Harleen Kaur [1,*], Elisa Vilvert [1,*], Miguel Ángel Corrales Gutiérrez [1], Jiasui Zhan [1], Dimitar Douchkov [2], Francesca Desiderio [3], Heriberto Vélëz [1,4], Salim Bourras [1].

[1] Department of Forest Mycology and Plant Pathology. Swedish University of Agricultural Sciences. Almas Allé 5, 750 07, Uppsala, Sweden.

[2] Leibniz-Institute of Plant Genetics and Crop Plant Research, 06466-Gatersleben, Germany.

[3] Council for Agricultural Research and Economics (CREA) - Research Centre for Genomics and Bioinformatics, Fiorenzuola d'Arda, Italy

[4] Current address: College of Science, Mathematics and Technology. Wenzhou-Kean University. 88 Daxue Rd, Ouhai, Wenzhou, Zhejiang Province 325060, China.

Institute X, Department X, Organization X, City X, State XX (only USA, Canada and Australia), Country

[2]Laboratory X, Institute X, Department X, Organization X, City X, State XX (only USA, Canada and Australia), Country

*** Correspondence:**
Dr. Heriberto Vélëz

hvelez@kean.edu

Prof. Dr. Salim Bourras

salim.bourras@slu.se

Keywords: wheat, Fusarium head blight, FHB, leaf botch, mycobiome

Abstract

Increasing the durability of crop resistance to plant pathogens has become a major concern in plant pathology. There are 32 diseases of agronomical importance in wheat, which makes disease management in this crop of worldwide importance extremely challenging. Two important groups of wheat pathogens driving the consumption of chemical fungicides in Sweden and worldwide are those causing head blight diseases and leaf blotch diseases. Swedish fields are regularly infested with head blight diseases typically driven by a complex of *Fusarium* and non-fusarium taxa including *F. graminearum*, *F. culmorum*, while leaf blotches are typically caused by *Zymoseptoria tritici*, *Pyrenophora tritici-repentis*, and *Parastagonospora nodorum*. In this work, we present a survey of the larger diversity of taxa associated with head blight and leaf blotch diseases in Sweden, with the primary aim to assess the usefulness of such an approach to develop new understanding and tools for disease diagnostics and management *sensu lato*. Here, we analyze nearly a thousand isolates collected from wheat fields across eight counties in Sweden and report the identification of pathogenic and non-pathogenic taxa as well as candidate biological control agents associated with head blight and leaf blotch diseases. We argue that such surveys represent an important tool for improving disease diagnostics, disease forecasting, and integrated management in wheat.

Introduction

Disease identification in the field can be very challenging, considering the complexity and the convergence of symptoms caused by different pathogen species. For diseases typically caused by a complex such as Fusarium Head Blight (FHB), several fungal species can be implicated. For instance, there are 17 *Fusarium* sp. and non-*Fusarium* species implicated in FHB. Of these, *F. graminearum* and *F. culmorum* are often presented as the most important drivers of the disease, with F. *graminearum* often being the most predominant species (**Karlsson et al., 2021**). The composition of the complex can significantly vary among countries depending on the varieties grown in the field, agricultural practices, or climate (**Karlsson et al., 2021**). For instance, a field monitoring study conducted by Xu et al. (2005) in four European countries (Hungary, Ireland, Italy, and the UK), it was shown that FHB was frequently associated with *F. graminearum* and *F. poae* in Italy and Hungary but not in Ireland and the UK, while *F. culmorum* was rarely detected except in Ireland (**Xu et al., 2005**). This demonstrates the importance of regularly monitoring FHB for the correct identification of the causal agents and proper assessing the efficiency of management strategies.

Other prominent examples of phenotypic complexity are leaf blotch diseases caused by *Zymoseptoria tritici*, *Pyrenophora tritici-repentis*, and *Parastagonospora nodorum*. All pathogens cause convergent disease symptoms that can be confounded with each other. Actually, the three pathogen species were historically confounded as one species, then *Z. tritici* and *P. nodorum* were referred to as the Septoria blotch complex or Septoria complex due to frequent co-occurrence of the two species and the similarity of symptoms. From a resistance breeding perspective, the distinction between those three species is crucial since it was shown that the host resistance is genetically different (i.e., requires different resistance genes, resistance mechanisms, and breeding strategies) (**Brown et al., 2015**). This further demonstrates the importance of monitoring and precise disease diagnostics as a tool for disease management. Furthermore, leaf blotch diseases in wheat are still largely controlled with fungicides, leading to the rapid development of fungicide resistance in pathogen populations across Europe (**Pereira et al., 2020; Justesen et al., 2021; Jørgensen et al., 2021, Jørgensen et al., 2022**) Thus, surveys are essential for the management of fungicide resistance and further highlight the importance of continuous isolation and characterization of pathogen populations from the field.

69 One major challenge for disease diagnosis in wheat is the recurrent emergence of hypervirulent
70 pathogen races, with one prominent example being the stem UG99 from the wheat pathogen *Puccinia*
71 *graminis* f. sp. *tritici*, that was responsible for a global pandemic of stem rust in wheat (**Singh et al.,**
72 **2011**). From a phenotypic perspective, it is impossible to distinguish the stem rust symptoms caused
73 by the UG99 race from any other race, thus highlighting the importance of molecular race
74 characterization for proper monitoring and resistance breeding (**Patpour et al., 2022**). A similar
75 challenge is imposed by *Blumeria graminis* f.sp. *triticale* (*B.g. triticale*), a new wheat pathogen that
76 emerged from the hybridization of wheat powdery mildew (*B.g. tritici*) and rye powdery mildew (*B.g.*
77 *secalis*) (**Menardo et al., 2016**). *B.g. triticale* is a new pathogen with an expanded host range that can
78 not only infect the Triticale crop but also wheat, causing symptoms that are indistinguishable from the
79 native wheat powdery mildew species *B.g. tritici* (**Menardo et al., 2016**) These examples further
80 demonstrate the importance of monitoring and the molecular identification of the causal agent as a tool
81 for the surveillance of emerging and re-emerging diseases.

82

83 The wheat mycobiome has been shown to be an important source of beneficial fungal endophytes with
84 promising biological control properties. Such antagonists often occur in the same ecological
85 niches/tissues as their 'target' pathogen species and have thus been isolated from various organs,
86 including roots, leaves, seeds, or ears (**Huang & Pang, 2017; Yue et al., 2018; Rojas et al., 2020**).
87 Considering the genetic diversity of the endophytic taxa inhabiting wheat, only a fraction of the wheat
88 mycobiome has been characterized for its biological control properties. Such work is mainly restricted
89 by the tedious initial isolation and molecular characterization of hundreds (if not thousands) of fungal
90 taxa. We, therefore, argue that surveys for diseases could be coupled with surveys for biological control
91 agents, taking advantage of the availability of host tissues where both pathogens and potential
92 antagonists can be isolated. In this study, we aimed to provide an experimental proof-of-concept for
93 the possible uses of disease sampling and monitoring campaigns for constructing a wheat mycobiome
94 library that can be used to understand and monitor wheat head blight and leaf blotch diseases in
95 Sweden. In particular, we assess if such a library can inform on shifts in pathogen populations and
96 possibly lead to the identification of potential emerging diseases and candidate biological control
97 agents.
98

Materials and methods

Sample collection and handling

A survey of wheat diseases was conducted in collaboration with the plant protection extension services of the Swedish Board of Agriculture. In 2020, spikes were collected from spring wheat varieties cultivated in Sweden and grown in a small propagation plot north of Stockholm. The plot consisted of the six Spring wheat varieties: Alderon, Dacke, Dala, Happy, Rohan, Stanley; two spring wheat genotypes used as scientific standards: Bobwhite and Fielder; and one triticale genotype. In 2021 and 2023, spike and leaf samples were collected by field pathologists from the plant protection extension services from eight counties across Sweden: Norrbotten, Uppsala, Stockholm, Södermanlands, Östergötland, Västra Götaland, Gottland, and Skåna (Figure 1 A). Samples were typically shipped within 24 hours in glycine bags and immediately processed or stored at 4°C in dry storage until further processing.

Media preparation for isolation and long-term conservation

Two different media were used for pathogen isolation, purification, and long-term storage. Potato dextrose agar (PDA) was prepared from dehydrated pre-mixed media from MP Biomedicals (USA) according to the manufacturer's instructions. Yeast malt sucrose (YMS) agar medium was prepared by mixing solve 4 g yeast extract, 4 g malt extract, and 4 g sucrose, and 16 g agar in 1000 ml milliQ water, then autoclaving for 5 min at 121°C. For mid-term storage, isolates were kept as slow-growing cultures on half-strength PDA or YMS agar in small glass vials and stored in the dark at 4°C. For long-term storage, three to four ca, 5mm mycelial plugs were cut from a growing colon, placed in a 2ml cryotube containing 30% glycerol, and stored at -80°C. For *Z. tritici*, long-term storage vials were prepared from liquid cultures as previously described by Fagundes and collaborators (**Fagundes et al., 2020**).

Isolation and purification of fungal colonies from spikes and leaves

Seeds and glumes were manually separated from full spikes and surface sterilized under a sterile hood for one minute in 1% sodium hypochlorite, followed by 30 seconds in 70% ethanol, and washed twice for 30 seconds in autoclaved Milli-Q water. Individual seeds were placed in Petri plates containing fungal culture media amended with 50 µg/ml of Kanamycin. For leaf segments a square of ca 5mm width was dissected around blotch symptoms typically consisting of necrotic spot often surrounded by

129 a chlorotic ring. Segments were surface sterilized under a sterile hood for 30 seconds in sodium
130 hypochlorite, followed by 30 seconds in 70% ethanol, and washed twice for 30 seconds in autoclaved
131 Milli-Q water. Three samples from the same leaf were placed in Petri plates containing fungal culture
132 media amended with 50 µg/ml of Kanamycin. Alternatively, samples were also simply washed in Milli-
133 Q water and further processed into plating. All plates were incubated at 20°C until colonies were visible
134 (usually around 5 to 7 days). Individual colonies were picked and transferred to new plates and
135 incubated at 20°C. The process was repeated until a single pure colony was obtained. For the specific
136 case of *Z. tritici*, leaf segments harboring pycnidia were incubated at 18°C in a humid chamber
137 consisting of a Petri dish supplemented with a sterile absorbent paper disk soaked with sterile water.
138 Plates were inspected every day under a binocular to search for bursting pycnidia where mucilage had
139 been ejected. In such a case, the pycnidium was carefully fetched using a sterile needle under a
140 binocular placed inside a sterile hood and transferred into a Petri dish with YMS agar, supplemented
141 with 50 µg/ml of Kanamycin.

142

143 **DNA extraction and genotyping by fragment sequencing**

144 A modified cetyltrimethylammonium bromide (CTAB) based DNA extraction method was used to
145 extract DNA of fungal isolates. Briefly, mycelium plugs were used to inoculate a liquid medium
146 containing malt extracts and vitamins (MEV). Cultures were incubated with ca. 150rpm shaking in the
147 dark at 25°C for two weeks. Then, mycelium was harvested, homogenized with a CTAB buffer (3%
148 CTAB; 150 mM TRIS-HCl; 2.6 M NaCl; 20 mM EDTA), and incubated at 65°C for 30 min inside a
149 water bath. The samples were centrifuged at 10’000 g for 10 min and the supernatant was transferred
150 to a new tube supplemented with an equal volume of chloroform. After a second centrifugation at
151 10’000 g for 10 min, the supernatant was transferred to a new tube, an equal amount of isopropanol
152 was added, and the mix was incubated at -20°C for a few minutes. A final centrifugation at 10’000 g
153 for 10 min resulted in the deposition of a DNA pellet, which was washed using 70% ethanol and
154 resuspended in TE buffer. In addition, another DNA extraction method was used to extract the DNA
155 of the fungal isolates. First, mycelium plugs from the isolates were cultured in falcon tubes containing
156 10 ml of YMS liquid medium and incubated for 7-15 days at 150 rpm and 25 °C in dark. Then, the
157 mycelium was harvested, freeze-dried, and subjected to genomic DNA extraction using the Nucleo
158 Mag Plant kit (Macherey-Nagel GmbH &Co. KG, Germany) in the automated nucleic acid extractor
159 Maelstrom 4800 (TANBead Taiwan Advanced Nanotech Inc., Taiwan).

160

161 Identification of pathogen species was carried out by Polymerase Chain Reaction (PCR) of the genomic
162 DNA followed by amplicon sequencing of conserved nuclear locus, internal transcribed spacer (ITS)
163 rDNA. For ITS PCR, primer pair ITS1 (5'- TCCGTAGGTGAACCTGCGG-3') and ITS4 (5-
164 TCCTCCGCTTATTGATATGC-3') were used for genotyping (**White T.J., 1990**). PCR amplification
165 was followed by PCR clean-up using exonuclease kit (Thermo Fisher Scientific) according to the
166 manufacturer's instructions. Amplicons were subsequently sent for fragment sequencing at Macrogen
167 Europe (The Netherlands, https://www.macrogen-europe.com/). DNA sequences were manually
168 curated and analyzed for sequence homology to fungal sequences deposited at the National Center for
169 Biotechnology Information (NCBI) using the BLASTn search tool. Isolates used for leaf infection
170 assays were also tested with *F. graminearum* marker GOFW (5'-
171 ACCTCTGTTGTTCTTCCAGACGG-3') GORV (5'- CTGGTCAGTATTAACCGTGTGTG-3') (de
172 Biazio et al., 2008), and for *F. culmorum* with Fc03 (5'-TTCTTGCTAGGGTTGAGGATG-3') Fc02
173 (5'-GACCTTGACTTTGAGCTTCTTG-3') (**Astrid Bauer and Seigner, 2015**).

174

175 **Plant cultivation and infection assays**

176 Wheat plants were grown in the phytotron (controlled climate chambers) for three to four weeks at
177 20°C, 70% relative humidity and 300µMOL light intensity. The inoculum was composed of isolate
178 HK48 (*Fusarium graminearum*), HK50 (*Fusarium culmorum*). The isolates were incubated for two
179 weeks at 25°C and constant darkness on OMA. The conidia were scraped from the colony surface and
180 resuspended in sterile water. The inoculum cell density was adjusted to 250 spores per µl using water.
181 Leaf inoculation was based on a protocol originally developed at the Leibniz Institute of Plant Genetics
182 and Crop Plant Research and adapted to our conditions. Three- to four-weeks-old wheat leaves were
183 randomly selected and cut into 4 cm lengths. A hole was punctured in the middle of the leaf segment
184 and inoculated with a 30 µl spore suspension. Three biological replicates consisting of each of two
185 technical replicates were inoculated with either *F. graminearum* or *F. culmorum*. A total of 360 leaf
186 segments were placed in water agar and incubated in phytotron for four days. The necrosis was
187 observed in each of the 360 leaf segments and scored visually.

188

189 **Image analysis and morphotyping**

190 Isolate pictures were analyzed using the open-source Fiji from ImageJ (**Schindelin et al., 2012**). To
191 minimize noise from the background, the region of interest (ROI) was defined manually with the circle
192 tool and added to the ROI manager ("Analyze/Tools/ROI manager/Add" and "Edit/Clear outside").
193 Once the ROI was defined, general color data was extracted ("Analyzed/color histogram"). After this
194 first step, the image was split into three different channels (blue, green, and red), and the different
195 features of interest were extracted for each channel ("ROI manager/Measure"). To proceed with texture
196 analysis of each channel image, we analyzed the image with the GLCM texture macro, defining the
197 size of the step in pixels as 1 and the direction of the step as 0 degrees ("Plugins/GLCM texture").
198 Finally, the image type was changed to 32-bit ("Image/Type/32-bit") to perform the last step of the
199 analysis. We selected *SurfCharJ1q* macro ("Plugins/ SurfCharJ1q") to analyze roughness features. At
200 the end of the analysis, each sample had 90 different variables to be studied.

201

202 **Statistical analysis**

203 All statistical analyses were performed with R (version 4.2.2.) in Rstudio environment (**R Core Team,**
204 **2021**). The packages used for the analyses were: *caret, cluster, corrplot, datawizard, factoextra,*
205 *faraway, readxl,* and *stats*. Data collected from ImageJ was normalized throughout the Z-scoring
206 transformation. After data transformation, a linear model was adapted to analyze the putative
207 correlation among the studied variables. Variables without changes among samples or with a
208 correlation coefficient above 0.9 were removed. After this first filtering step, we performed a second
209 selection, deleting variables with the highest correlation coefficients and variance inflation factors
210 (VIF) values. Principal Component Analysis (PCA) was performed with the filtered and normalized
211 data. To perform clustering analysis, agglomerative nesting (AGNES) and divisive analysis (DIANA)
212 algorithms were applied for hierarchical clustering over our filtered data. Finally, *kmeans* and *medoids*
213 analysis was performed with a predefined number of clusters of 2. *Kmeans* analysis was performed
214 with *Hartigan* and *Wong* algorithm and Euclidean distance was selected for *medoids* analysis. The
215 aggregation level of each cluster was measured throughout their silhouette value.

216

217

Results

Overall diversity of the wheat mycobiome library

In this study, hundreds of colonies were isolated from spikes and leaves collected over three field campaigns in eight counties across Sweden (Figure 1A). Of these, several isolates did not make it to the final set due to practical issues with growth, bacterial contaminations, failure of the genotyping at the PCR or the fragment-sequencing step. Still, we were able to recover a final set of 940 successfully genotyped samples which was the basis for the following analyzes. First, we concatenated all the genotypic data and evaluated the overall diversity of the resulting fungal collection in terms of genus diversity (Figure 1B). Here, it is important to read the following primarily in terms of qualitative diversity, considering the inherent bias due to the isolation method, and where abundance is primarily meant in terms of frequency of isolation. We were able to recover taxa from 14 different genera with a minimum of two representative (i.e. independently recovered isolates). Of these, the most abundant genera included *Fusarium* sp., the ubiquitous *Alternaria* sp., and to a lesser extent *Zymoseptoria* sp., *Pyrenophora* sp., *Microdochium* sp., and *Parastagonospora* sp., which is consistent with the fact that the sampling was mainly targeted to FHB, Leaf Blotch diseases of wheat. We therefore conclude that the resulting isolate library is relevant to the diseases covered by the survey.

We then assessed the species diversity of the two most abundant taxa, namely, *Fusarium* sp. and *Alternaria* sp (Figure 1C, 1D). We found that the most abundant Alternaria species were *A. infectoria*, and *A. alternata*, which are commonly associated with head diseases such as the wheat black point, and also to mycotoxin production (**DeMers M., 2022**). (Figure 1C). For *Fusarium* sp., we were able to recover a diversity of taxa typically associated with FHB in wheat, with the most common species including *F. culmorum*, *F. graminearum*, *F. poae*, and *F. avenaceum* (Figure 1D). We conclude that the collected data indicate a large diversity of taxa typically implicated in head diseases of wheat present in Swedish wheat fields, representing a potential risk for disease outbreaks.

Finally, we assessed the overall diversity of the library in terms of the representation of disease-causing agents as well as potential antagonists potentially corresponding to candidate biological control agents. We reasoned that biological control agents often co-exist with their targets in the same ecological niches and may thus be co-isolated from the same tissues. The library contained 23 different fungal taxa commonly implicated in wheat diseases affecting the seeds, the leaves, and the spikes; which is

249 consistent with the wheat organs/tissues surveyed in this study (Table 1A, 1B). We also note that head
250 blight and leaf blotch diseases are well represented in this list which is again in line with the aim of
251 this survey. Of these, two species, *Nigrospora oryzae* and *Stemphylium vesicarium*, have been
252 described as potentially new wheat pathogens (**Liu et al., 2021, Mohamed et al., 2022**), which we
253 have classified as candidate emerging diseases for surveillance (Table 1B). We also found eight taxa
254 that may represent potential biological control agents which were assigned based on previous studies
255 (Table 1C). We argue that such isolates represent an added value for the survey aiding the identification
256 of potentially beneficial microorganisms that could be evaluated for their biological control properties.

257

258 **Inventory of pathogenic and endophytic isolates associated with Leaf Blotch in Sweden.**

259 For the leaf mycobiome associated with Leaf Blotch diseases, we recovered isolates from typical blotch
260 symptoms as well as from symptomless tissues. We deduced that symptomless tissues may be the
261 habitat for endophytic fungi that could be antagonistic to the pathogenic taxa or harbor pathogens
262 surviving as silent endophytes.

263

264 Overall, *Alternaria* species dominated the infection, which is consistent with the fact that they are
265 known to be ubiquitously found as weak pathogens or saprophytes on different plant tissue (Figure
266 2A). *Alternaria* sp. apart, the most frequently isolated species were *Zymoseptoria tritici*, *Pyrenophora*
267 *tritici-repentis*, and *Parastagonospora nodorum*, all of which being prominent causal agents of blotch
268 diseases in wheat. We here conclude that the collection isolated from leave does represent the diseases
269 targeted by the survey. We then differentiated the isolates recovered from typical blotch symptoms
270 (Figure 2B), from those recovered from symptomless tissues (Figure 2C). *Alternaria* sp. apart, *Z. tritici*,
271 *P. tritici-repentis*, and *P. nodorum* were the most frequently isolated species from blotch symptoms.

272

273 Interestingly, we have also isolated taxa typically implicated in FHB, including *F. culmorum*, *F.*
274 *graminearum*, and *Microdochium nivale*. In comparison, the most frequently isolated taxa from
275 asymptomatic tissues apart from *Alternaria* sp. (i.e. surviving as silent endophytes) were *P. tritici-*
276 *repentis*, and *P. nodorum*, but also *Z. tritici*, and *M. nivale*. This data indicate that members of the FHB
277 complex can possibly survive as silent endophytes in the leaves and potentially cause blotch-like
278 symptoms that can be confound with the typical blotch pathogens *Z. tritici*, *P. tritici-repentis*, and *P.*
279 *nodorum*.

280

281 We also tested the capacity of *F. culmorum*, *F. graminearum* to cause blotch-like symptoms on wheat
282 leaves. To do so, we performed point inoculation of leaf segments harvested at the seedling stage and
283 visually assessed the development of necrotic lesions (see Methods). We inoculated 30 commercial
284 spring wheat cultivars commonly grown in Sweden (Figure 2D, 2E). We found that *F. culmorum*
285 caused necrotic lesions on at least 5 out of the 30 commercial cultivars tested (Figure 2D), while *F.*
286 *graminearum* caused necrotic lesions on 15 commercial cultivars (Figure 2E). These results
287 substantiate the hypothesis that *F. graminearum* and *F. culmorum* can potentially cause leaf blotch-
288 like symptoms in Swedish fields on several of the commonly grown spring wheat varieties.

289

290 **Inventory of pathogenic and endophytic isolates associated with FHB in Sweden**

291 For the spike mycobiome, we recovered isolates from seeds as well as from glumes and searched for
292 both pathogenic and non-pathogenic taxa. Our reasoning was that glumes may offer a secondary habitat
293 for wheat ear pathogens or potential antagonists competing for the same ecological niche in the seed
294 vicinity. In contrast to the leaf mycobiome, *Fusarium* species dominated over *Alternaria* sp., including
295 the two most important causal agents of FHB, namely *F. culmorum* and *F. graminearum* (Figure 3A).
296 In addition, several typical members of the FHB complex were isolated, including *F. poae*, *F.*
297 *avenaceum*, *F. equiseti*, and *M. nivale*. We then investigated the differences in the qualitative diversity
298 between the taxa recovered from seeds vs. glumes (Figure 3B, 3C). Interestingly, the less pathogenic
299 taxa *F. poae* and *F. avenaceum* were mainly isolated from seeds (Figure 3B), while the more
300 pathogenic taxa *F. graminearum* and *F. culmorum* were isolated from both seed compartments but
301 dominated in the glumes (Figure 3C). This data suggests that *Fusarium* species implicated in FHB
302 fully occupy the seed habitat, with the glumes possibly acting as a secondary niche where pathogenic
303 taxa seem to outcompete other fungal taxa, such as *Alternaria* sp which has been isolated ubiquitously
304 from all tissues analyzed in this study except glumes.

305

306 We then expanded this analysis to possible differences between cultivars. We used a subset of samples
307 recovered from a small propagation plot, where isolations were exclusively carried out with seeds.
308 First, we concatenated the data by cultivar and genus/species with at least two representatives (Figure
309 3D), and then we grouped the species into representatives of common head diseases (Figure 3E).
310 Additionally, we also included isolates from *Epicoccum* sp. which we could isolate from leaves, but

311 also and mostly from seeds. Our reasoning was that *Epicoccum* sp. had been previously described as
312 being associated with FHB; however, while a role as a possible antagonist/biocontrol agent has been
313 suggested (**Karlsson et al., 2021**), its contribution to the FHB complex is still poorly understood. We
314 found that *Alternaria* sp. could be isolated from most, if not all, cultivars, which is consistent with their
315 characteristic as ubiquitous plant-associated fungi, sometimes acting as weak pathogens. However, the
316 distribution of *Fusarium* sp. and *Epicoccum* sp. was more scattered across cultivars (Figure 3E). When
317 grouped by common diseases, the results suggested that head mold disease seems to be a more
318 ubiquitous risk factor than head blight, although members of the FHB complex still infected 6 out of 9
319 tested cultivars.

320

321 We finally investigated the specific case of FHB-infected ears (Figure 3F) and leaves with typical
322 blotch symptoms that were collected from the most northern location in our study: Piteå (Norrbotten
323 county, Figure 1A). Interestingly, we mostly recovered *M. nivale* from the leaf blotch symptoms and
324 *F. avenaceum* and *M. nivale* from the FHB-infected ears (Figure 3G). These results suggest that in
325 these northern latitudes, blotch symptoms are probably cased by *M. nivale,* which is the common agent
326 of the Snow Mold disease of wheat, while FHB is possibly caused by the weaker pathogens *F.*
327 *avenaceum* and *M. nivale*. We conclude that such observations demonstrate the usefulness of such
328 surveys to shed light on possible changes in the disease landscape and alert on the possible re-
329 emergence of diseases.

330

331 **Morphotyping of *Fusarium* sp. and *Epicoccum* sp. isolates**

332 In a last series of analyses, we took advantage of the library to explore the possibilities of morphotyping
333 to rapidly sort and identify fungal species, with the prominent addition of modern image analysis
334 technologies. We inferred that the capacity to rapidly sort and classify fungal taxa as soon as they are
335 available as colonies growing on a plate will be a handy tool to accelerate and scale up the diagnostics,
336 which would also allow us to target specific taxa or specific morphotypes. To do so, we aimed to
337 provide a proof-of-concept using *Fusarium* sp. and *Epicoccum* sp. as targe taxa to differentiate solely
338 using imaging.

339

340 A pipeline was designed to extract different image attributes from the isolate pictures using advanced
341 functions in the imageJ image analysis suite (see Methods). A Principal Component Analysis (PCA)

342 showed that although the subset of selected image variables still shows some level of correlation
343 (Figure 4A), they can still explain 56.7 % of the observed variability (Figure 4B). The image features
344 with the highest contribution to the '*Dimension 1*' is the mean blue channel, and the blue and green
345 intensity density (Figure 4C), meanwhile the highest contributors to 'Dimension 2' are the minimum
346 green intensity and the FAD values for red, blue, and green (Figure 4D). These results suggest that the
347 selected characteristics could represent a balanced mathematical description of the distribution of our
348 samples. However, we cannot exclude further optimization considering the inherent correlation
349 between some visual features (such as color) and the fact that some image features contribute more to
350 the total variability. Finally, with this still basic analysis, we could delineate two clear but slightly
351 overlapped clusters (Figure 4B) differentiating *Fusarium* sp. from *Epiccocum* sp. isolates. In order to
352 improve the clustering of our data, we applied Agglomerative Nesting (AGNES) (Figure 4E) and
353 Divisive Analysis Clustering (DIANA) (Figure 4F) algorithms (see Methods). The AGNES algorithm
354 resulted in a dendrogram with an agglomerative coefficient of 0.78; meanwhile, the DIANA algorithm
355 gave a higher value of 0.82, suggesting a solid clustering structure in our sample distribution. Although
356 the clustering does not differentiate between different *Fusarium* sp. species, the distribution shows that
357 we can reasonably differentiate between the genus *Epicoccum* sp. and *Fusarium* sp. with only six
358 miscalls.

359

360 Considering the quality of the data, we aimed at further clustering using *K-means* (Figure 5A) and
361 *Partition Around Medoids* (*PAM*) algorithms (Figure 5B), and calculated the average silhouette value
362 for each cluster created (Figure 5C, 5D). Although the global accuracy increased was improved to
363 0.918 (*K-means*) and 0.904 (*PAM*), we still had 6 miscalls with the *K-means* and 7 with the *PAM*,
364 which is consistent with the average silhouette value of 0.32 for the *K-means* clusters (Figure 5C) and
365 0.3 for the *PAM* clusters (Figure 5D). Interestingly, it seems that algorithms find it harder to
366 differentiate some *Epicoccum* sp. isolates from *Fusarium* sp. (*K-means*: 0.739, PAM: 0.739) while the
367 sensitivity for *Fusarium* (i.e. the capacity to properly identify *Fusarium* sp.) is higher in comparison
368 to *Epiccocum* (*K-means*: 0.980, PAM: 0.961. Therefore, despite the small dataset used in this analysis,
369 we could still provide proof of principle that imaging is a promising tool for advanced morphotyping
370 and the identification of specific fungi relevant to wheat.
371

372 **Discussion**

373 ***Wheat pathogens occupy a variety of tissues and niches***

374 In this study, we recovered typical wheat pathogens implicated in head blight and leaf blotch diseases
375 from a variety of tissues, including seeds, glumes, symptomatic leaf tissues, and asymptomatic leaves.
376 We had cases where *Fusarium* taxa typically implicated in FHB were isolated from blotch symptoms
377 in the leaves and other cases where typical blotch pathogens such as *P. tritici-repentis*, and *P. nodorum*
378 were isolated from wheat ears. Furthermore, typical leaf pathogens were also isolated as silent
379 endophytes from asymptomatic tissues. Fusarium species are well known as ubiquitous plant
380 colonizers that can survive in a variety of plant tissues and also in the soil (**Karlsson et al., 2021**). In
381 disease complexes such as FHB, where 17 different *Fusarium* and non-*Fusarium* taxa can be
382 implicated, the role of such secondary niches is poorly understood (**Karlsson et al., 2021**). From a
383 population perspective, the capacity of pathogens to survive in tissues or organs that are not their
384 primary habitat may increase the fitness of the pathogen population in the field by maintaining living
385 inoculum, throughout the field seasons and particularly when conditions are unfavorable. This was, for
386 instance, observed in the case of *Z. tritici*, where it was shown that avirulent isolates can still survive
387 and mate on resistant wheat hosts as symptomless endophytes or epiphytes (**Fones et al., 2023**), thus
388 contributing to pathogen fitness and adaptation through the maintenance of genetic diversity in the
389 field population. It was also shown that *Z. tritici* can induce systemic responses leading to whole plant
390 metabolic changes leading to increased susceptibility to secondary infection with a non-adapted
391 pathogen (**Seybold et al., 2020**). This is major because such mechanisms could also occur among
392 different isolates of the same pathogen population or different species of a disease complex, thus
393 providing a possible explanation for the functional relevance of secondary niches and the ubiquitous
394 nature of the taxa implicated in FHB.

395

396 ***The wheat mycobiome as a source for candidate biological control agents***

397 Microbial biological control agents are considered an important tool to reduce chemical inputs in crop
398 disease management. A variety of microbial agents with antagonistic properties against plant pathogens
399 has been described, and variety of mode of action underlying such effect has been reported including
400 antibiosis, parasitism, niche competition, or resistance priming in the host (**Köhl et al., 2019**).
401 Microbial biological control agents that correspond to naturally occurring competitors are commonly
402 found in the same ecological niches as their target pests. In this study, several candidate biological

403 control agents have been identified (Table 1C). For instance, strains of *Alternaria alternata* and
404 *Cladosporium cladosporioides* have been described as hyperparasite of the wheat stripe rust pathogen
405 *Puccinia striiformis* f. sp. *tritici,* (**Zheng et al., 2017; Zhang et al., 2022**). Similarly, *E. nigrum* has
406 been shown to a promising biological control agent against wheat stripe rust as well as *F. graminearum*
407 hile *Aureobasidium pullulans* and *Meyerozyma guilliermondii* has been described as biological control
408 agents against post-harvest Fusarium crown rot diseases, respectively (**El-Sharkawy et al, 2023;**
409 **Wachowska et al., 2016; Kthiri et al., 2021**). These results further demonstrate the usefulness of such
410 surveys in the broader context of IPM, by facilitating the identification of relevant candidate biological
411 control agents better adapted to the Swedish conditions.

412

413 ***Wheat disease diagnostics and its importance for management***

414 The beneficial vs. pathogenic lifestyle of a plant colonizing fungus can be determined mainly by the
415 host and the ecological niches it occupies. For instance, the biological control fungus *Clonostachys*
416 *rosea*, a naturally occurring root endophyte, has been shown to be effective against several foliar plant
417 pathogens. However, *C. rosea* has also been reported as the causal agent of root rot, crown rot, and
418 wilt-type diseases in garlic, faba bean, avocado, strawberry, sugar beet, and medicinal plants such as
419 *Angelica sinensis* and *Astragalus mongholicus* (**Ma et al., 2020; Qi et al., 2022; Diaz et al., 2022;**
420 **Afshari et al., 2017; Coyotl-Pérez et al., 2007; Zhang et al., 2022; Haque and Parvin, 2020,**
421 **Farhaoui et al., 2023**). Similarly, *E. nigrum* has been described as a potent biological control agent
422 against wheat stripe rust. However, *E. nigrum* is also the causal agent of the brown spot disease in
423 *Solanaceae* (**Jin et al., 2023**). These reports highlight the importance of continuous monitoring of field
424 populations and careful, systematic identification of the causal agents for identifying potential lifestyle
425 shifts in microbial populations.

426

427 Shifts from a beneficial endophytic lifestyle to pathogenicity through host switch, niche displacement,
428 and changes in the microbiome have been well documented for several prominent diseases such as
429 *Diplodia sapinea,* the causal agent of diplodia tip blight in Scots pine, and *Sarocladium oryzae* the
430 causal agent of rice sheet rot (**Blumenstein et al., 2022; Peeters et al., 2021**). Therefore, the
431 designation of beneficial endophyte/candidate biological control agents must be taken within the
432 context of the actual contribution of the species to the wheat mycobiome, meaning that both disease-
433 suppressing antagonistic and disease-promoting synergistic properties must be tested. This is directly

434 relevant to taxa such as *Epicoccum* sp. and *Alternaria* sp., considering their frequent association with
435 FHB and our poor understanding of how such mycobiome is assembled (**Karlsson et al., 2021; Schiro**
436 **et al., 2018; Nazabanita et al., 2022; Rojas et al., 2020**).

437

438 In this context, changes in the composition of the disease complex are also relevant, with the example
439 of FHB from Piteå, which seems to be caused by *F. avenaceum* and *M. nivale* (Figure 3F, 3G) and not
440 by *F. graminearum* and *F. culorum* as in the majority of the FHB tested samples (Figure 3A, 3B, 3C).
441 In contrast, we also recovered those typical FHB causal agents, *F. graminearum* and *F. culorum*, from
442 typical necrotic and chlorotic symptoms reminiscent of septoria leaf blotch diseases. These results
443 highlight the complexity of the wheat mycobiome and the limits of visual scoring considering the
444 complexity and often the convergence of disease symptoms caused by yet phylogenetically distant
445 taxa. We argue that such observations further highlight the importance of field surveys as a tool for
446 continuous identification and re-identification of the actual disease-causing agents present in the field.

447

448 ***A basis for targeted monitoring of potentially emerging wheat diseases***

449 The emergence of new diseases leading to global epidemics is relatively common in wheat, with stem
450 rust and wheat blast being two prominent examples. Wheat has also been the host for the emergence
451 of two new pathogens that did not existence before namely triticale powdery mildew and wheat blast.
452 Arguably, the large reservoir of wheat pathogens present in the agro-ecosystem is a challenge requiring
453 continuous monitoring for early detection of potentially new, emerging diseases. In this context, two
454 taxa identified in our survey are of particular interest: *N. oryzae*, and *S. vesicarium* (Table 1B). *N.*
455 *oryzae* is an ascomycete fungal pathogen and the causal agent of panicle branch rot disease on rice
456 (*Oryza sativa*) (**Liu et al., 2021**) In 2016, N. oryzae was reported to cause black lesions on the
457 hypocotyls of wheat seedlings in Kazakhstan, suggesting that some isolates of *N. oryzae* (a rice
458 pathogen) may have adapted to be pathogens on wheat, which is reminiscent of the emergence of wheat
459 blast (**Eken et al., 2016**). Smilarly, *S. vesicarium* has been reported to cause leaf spots on wheat in
460 Egypt (**Mohamed et al., 2022**), and to our knowledge, these pathogens have never been described in
461 Sweden before. We conclude that such results further highlight the relevance of this work since we can
462 now provide a rational basis for risk assessment and targeted disease monitoring of critical pathogens
463 in Swedish wheat fields.

464

465 **Author Contributions**

466 SB and HV led the research. SB, HZ, and JZ designed the research and developed the library. HK, EV,
467 MACG, HV, SB did laboratory experiments. HK, MACG, SB, DD, and FD developed infection assays.
468 MACG and SB developed the morphotyping. HK, EV, HV, and SB analyzed the genotyping data.
469 MACG performed statistical analyzes. MACG and SB edited the figures.

470

471 **Funding**

472 This was supported by funding from the Swedish Research Council for Sustainable Development
473 FORMAS (grant number 2020-01007) and the Carl Trygger Foundation (grant number 21:1171).

474 **Acknowledgments**

475 We would like to acknowledge the support of the Plant Protection Extensions 'Växtskyddscentralerna'
476 of the Swedish Board of Agriculture 'Jordbruksverket' (https://jordbruksverket.se/) with field sampling
477 across Sweden. We would like to thank Anders Lindgren, Lina Norrlund, and Elizabeth Lovetta for
478 supporting and coordinating sample collection and shipment. We thank Eula Gems Oreiro, Björn
479 Andersson from the Department of Forest Mycology and Plant Pathology (SLU) for their help handling
480 blotch infected samples and their contribution to maintaining the library. We also thank Fredric
481 Hedlund and Ayano Tanaka for their technical assistance with the growth facilities and the SLU
482 BioCentrum. We finally thank Katarina Ihrmark and Maria Jonsson for their technical assistance.

483

484

485 **Figures**

486

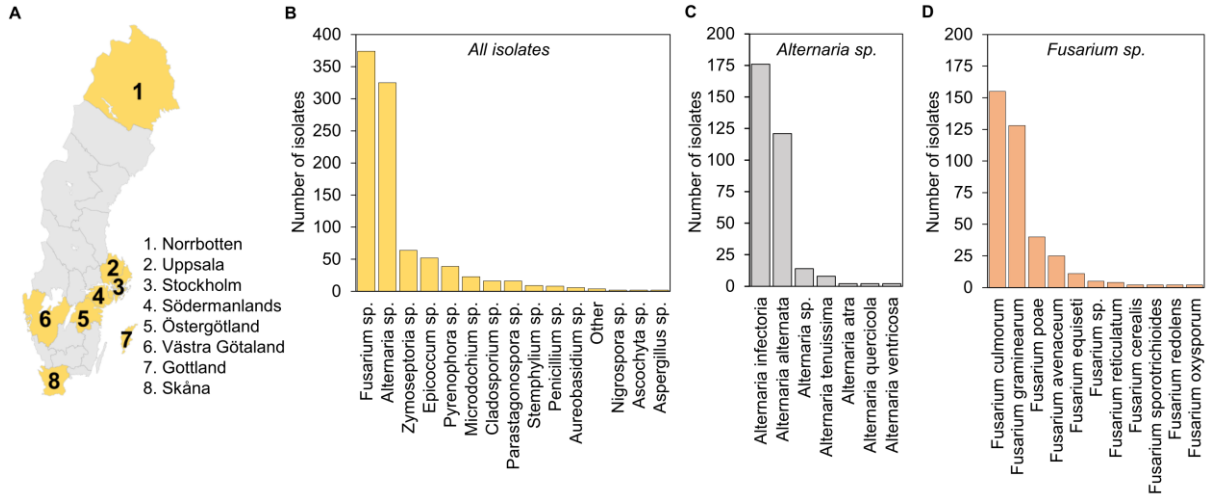

487

488 **Figure 1**. Summary and overall diversity of the wheat mycobiome library

489 (A) Geographical origin of the samples. (B) Overall diversity of the fungal genera represented in the library. (C)
490 Analysis of species diversity of *Alternaria* sp. (D) Analysis of species diversity of *Fusarium* sp.

491

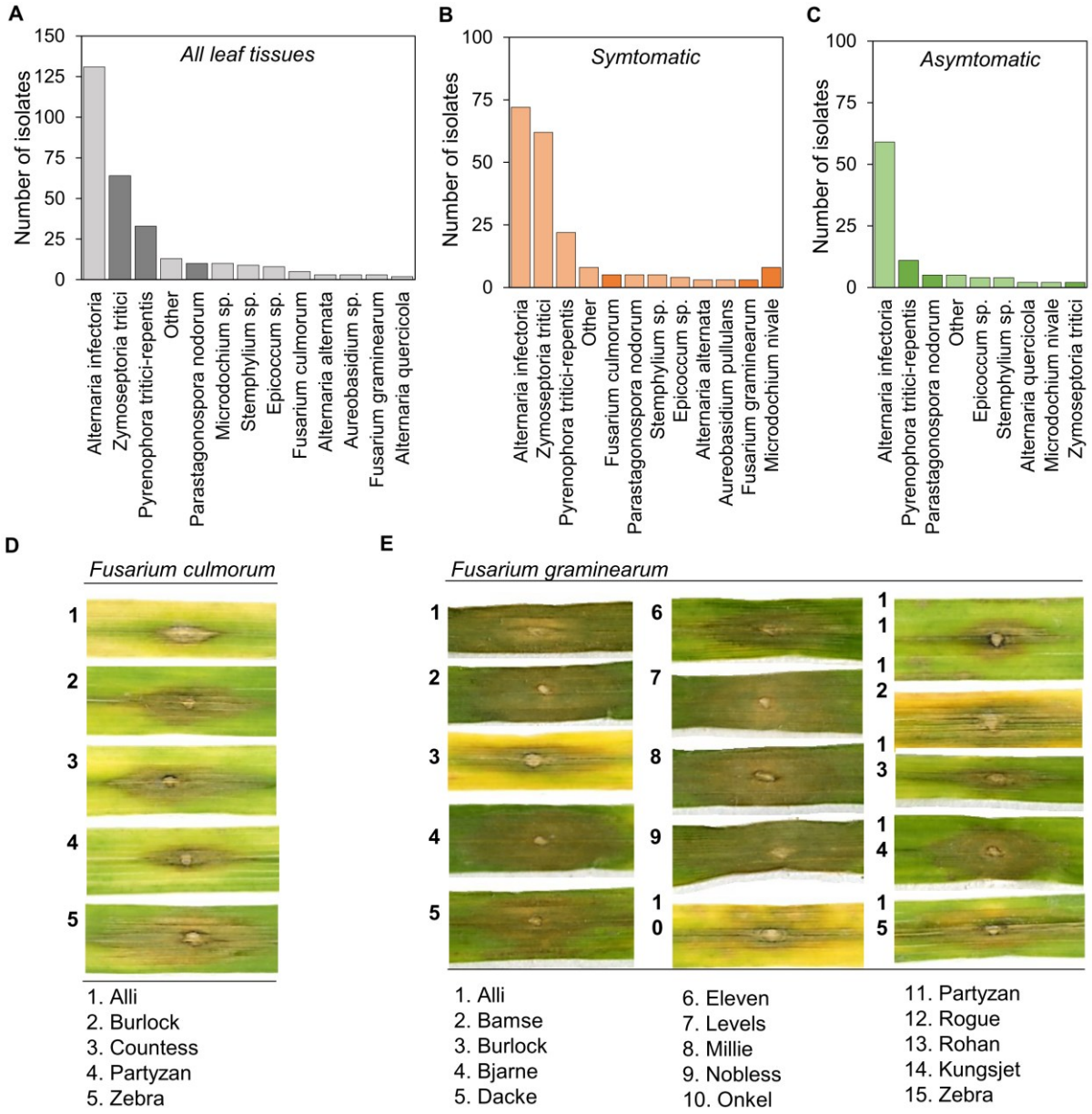

Figure 2. Summary of the wheat leaf mycobiome

(A) Overall diversity of the fungal taxa isolated from leaf tissues. (B) Summary of the fungal taxa recovered from tissues with typical leaf blotch symptoms. (C) Summary of the fungal taxa recovered from asymptomatic tissues from leaf blotch infected material. (D) Point leaf inoculations of different spring wheat commercial cultivars with *Fusarium culmorum* (see Methods). (E) Point leaf inoculations of different spring wheat commercial cultivars with *Fusarium graminearum* (see Methods).

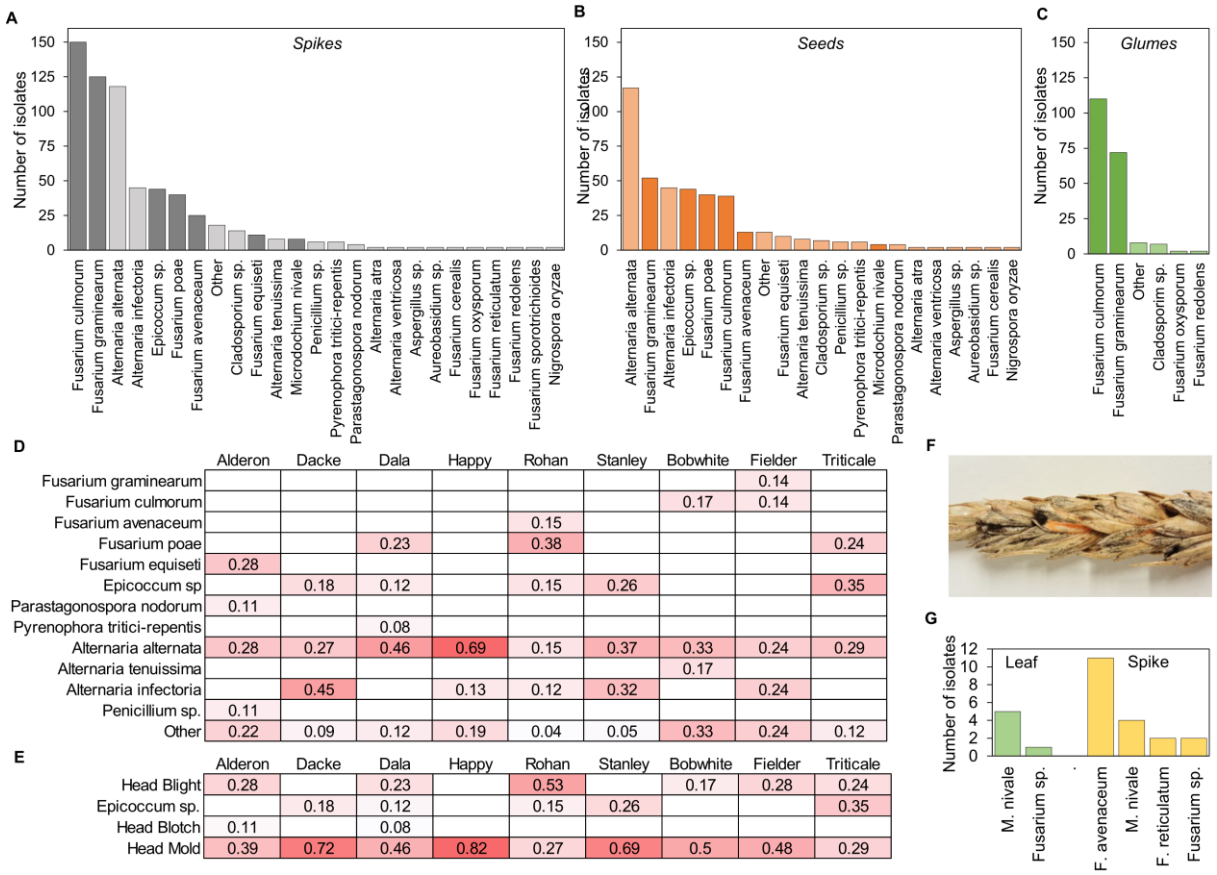

Figure 3. Summary of the wheat head mycobiome

(A) Overall diversity of the fungal taxa isolated from spikes. (B) Summary of the fungal taxa recovered from seeds. (C) Summary of the fungal taxa recovered from glume tissues. (D) Analysis of possible association between fungal taxa and wheat cultivars. (E) Analysis of possible association between common head diseases and wheat cultivars. (F) Photograph of typical Fusarium Head Blight symptoms on a wheat spike collected from the most northern location in our survey: Piteå. (G) Summary of the fungal taxa isolated from typical leaf blotch and head blight symptoms from samples collected in Piteå.

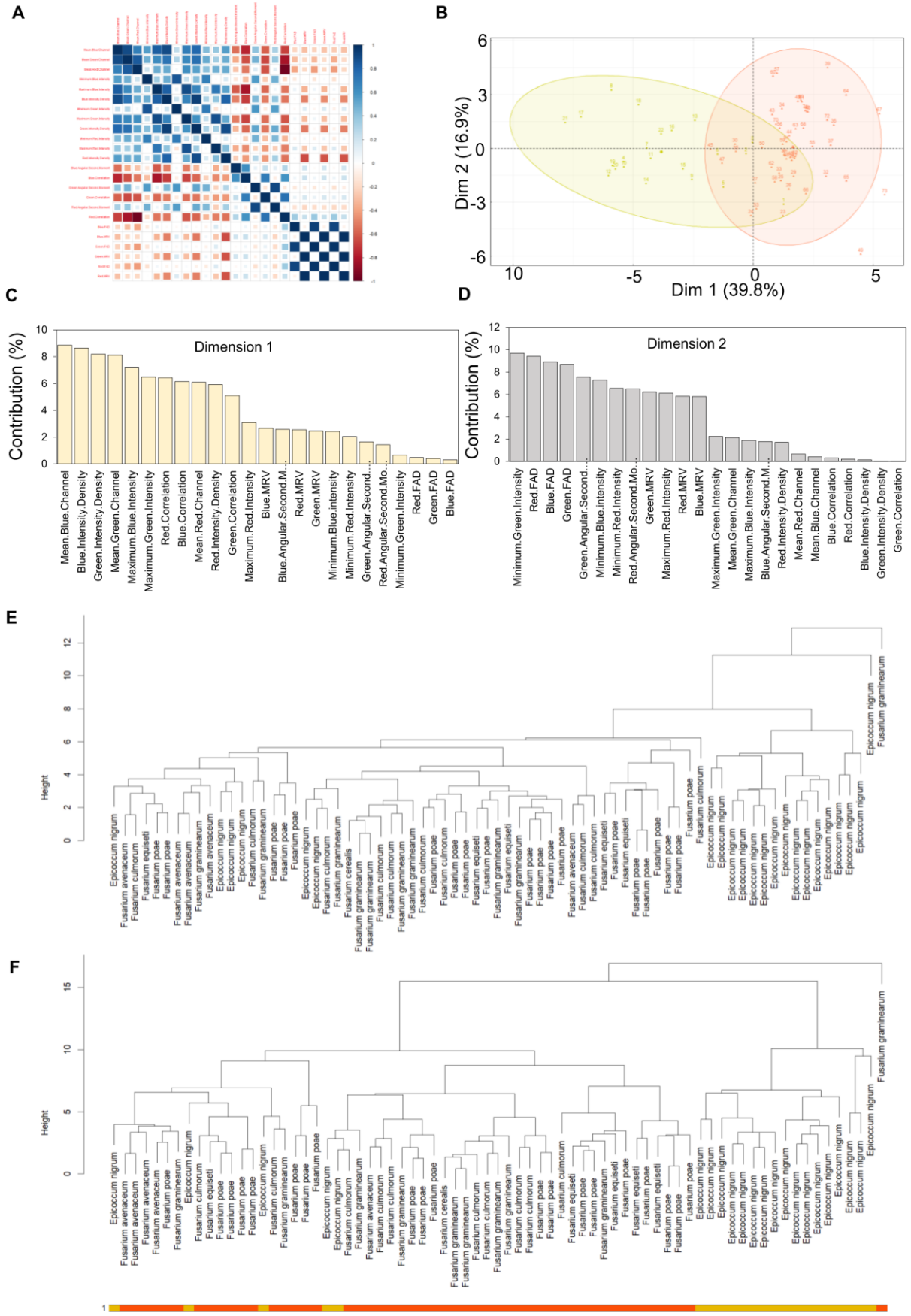
A
B
Dim 2 (16.9%)
Dim 1 (39.8%)
C
Contribution (%)
Dimension 1
Mean.Blue.Channel
Blue.Intensity.Density
Green.Intensity.Density
Mean.Green.Channel
Maximum.Blue.Intensity
Maximum.Green.Intensity
Red.Correlation
Blue.Correlation
Mean.Red.Channel
Red.Intensity.Density
Green.Correlation
Maximum.Red.Intensity
Blue.MRV
Blue.Angular.Second.M...
Red.MRV
Green.MRV
Minimum.Blue.intensity
Minimum.Red.Intensity
Green.Angular.Second...
Red.Angular.Second.Mo...
Minimum.Green.Intensity
Red.FAD
Green.FAD
Blue.FAD
D
Contribution (%)
Dimension 2
Minimum.Green.Intensity
Red.FAD
Blue.FAD
Green.FAD
Green.Angular.Second...
Minimum.Blue.intensity
Minimum.Red.Intensity
Red.Angular.Second.Mo...
Green.MRV
Maximum.Red.Intensity
Red.MRV
Blue.MRV
Maximum.Green.Intensity
Mean.Green.Channel
Maximum.Blue.Intensity
Blue.Angular.Second.M...
Red.Intensity.Density
Mean.Red.Channel
Mean.Blue.Channel
Blue.Correlation
Red.Correlation
Blue.Intensity.Density
Green.Intensity.Density
Green.Correlation
E
Height
F
Height

509

510 **Figure 4.** Feature extraction for morphotyping and dendrogram classification

511 (A) Correlation matrix of selected variables for image analysis of *Epicoccum* sp. and *Fusarium* sp. blue color
512 (values close to 1) indicates positive correlation meanwhile red color indicates negative correlation. (B) Principal
513 component analysis plot of visual data extracted from *Epicoccum* sp. and *Fusarium* sp. Isolate images. The
514 color yellow represents *Epicoccum* sp. isolates and the red color represents *Fusarium* sp. isolates. Circles
515 represent putative clusters. Dimension 1 and dimension 2 separate isolates based in the values of 24 different
516 visual characteristics. (C) Weights of the main explanatory variables for the first PCA dimension. (D) Weights of
517 the main explanatory variables for the second PCA dimension. (E) Dendrogram clustered by AGNES algorithm
518 built with Unweighted Pair Group Method with Arithmetic Mean (UPGMA). (F) Dendrogram clustered by the
519 DIANA algorithm. The yellow color represents *Epicoccum* sp. isolates, and the red color indicates *Fusarium* sp.
520 isolates.
521

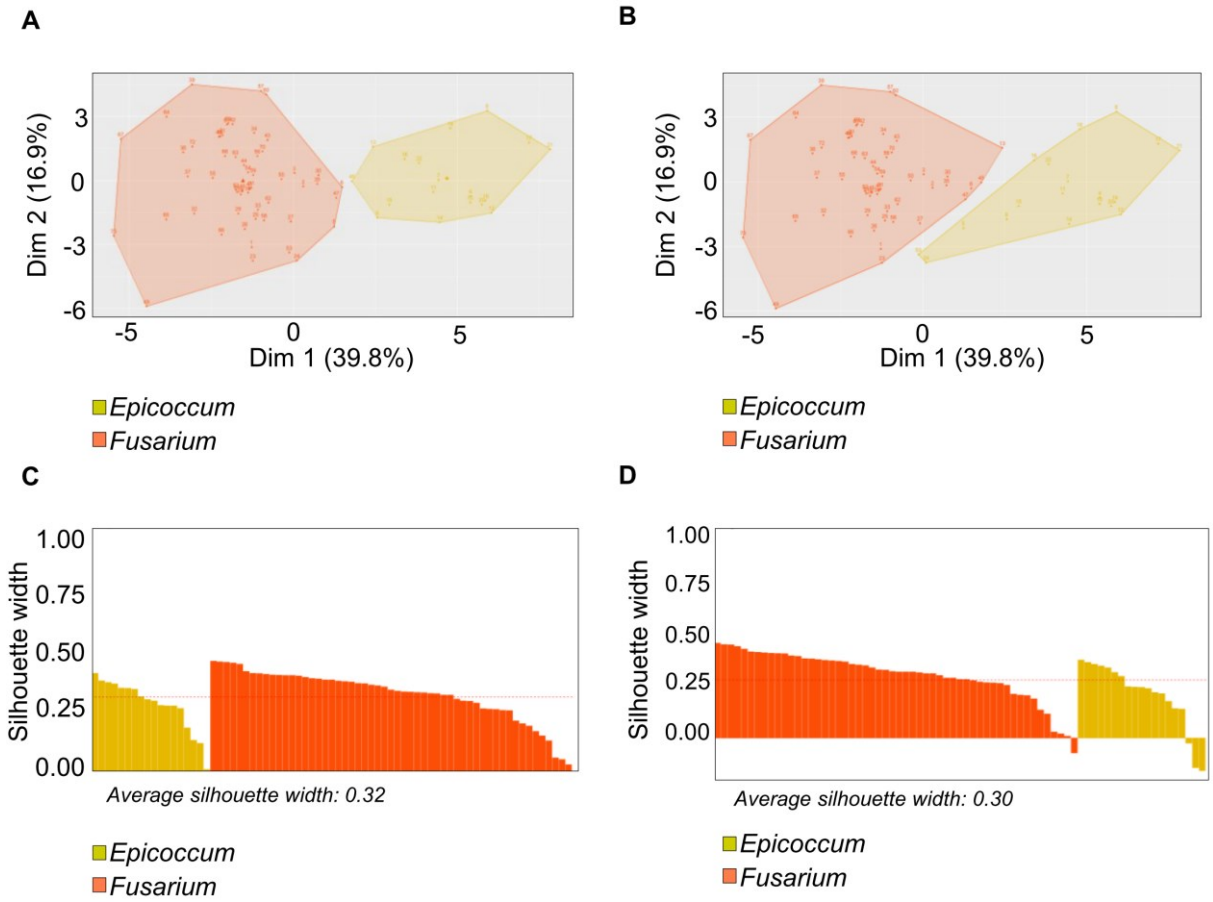

Figure 5. K-mean and PAM clustering of *Epicoccum* sp. and *Fusarium* sp. isolates

(A) Cluster analysis performed by K-means algorithm. The pre-selected number of clusters was defined as 2. Yellow represents the putative cluster for *Epicoccum* sp. isolates and red color represents the putative cluster for *Fusarium* sp. (B) Cluster analysis performed by PAM algorithm. The number of clusters was predefined as 2. Yellow area represents *Epicoccum* sp. isolates and the red area shows *Fusarium* sp. (C) Silhouette values for each isolate and average silhouette from cluster analysis with the K-means algorithm. (D) Silhouette values for each isolate and average silhouette from cluster analysis with the PAM algorithm. In (C) and (D) samples aggregated as *Epicoccum* sp. are represented with yellow bars meanwhile samples aggregated as *Fusarium* sp. are represented as red bars.

533 **Tables**

534 **Table 1.** Summary of possible contributions of different taxa to the wheat mycobiome.

Species	Predicted contribution	Reference
A. *Common wheat pathogens*		
Alternaria alternata	Black point	Somma et al. (2019)
Alternaria arborescens	Seed pathogen	Perello et al. (2016)
Alternaria infectoria	Black point	Somma et al. (2019)
Alternaria tenuissima	Black point	Disalov et al. (2015)
Fusarium acuminatum	Root rot	Mergoum et al. (1998)
Fusarium armeniacum	Head blight	Krone et al. (2021)
Fusarium avenaceum	Head blight	Karlsson et al. (2021)
Fusarium cerealis	Head blight	Leyva-Mir et al. (2022)
Fusarium culmorum	Head blight	Karlsson et al. (2021)
Fusarium equiseti	Head blight	Leyva-Mir et al. (2022)
Fusarium graminearum	Head blight	Karlsson et al. (2021)
Fusarium oxysporum	Wilt	Naguib et al. (2018)
Fusarium poae	Head blight	Karlsson et al. (2021)
Fusarium pseudograminearum	Crown rot	Kazan et al. (2017)
Fusarium redolens	Crown rot	Bozoglu et al. (2021)
Fusarium reticulatum	Head blight	Karlsson et al. (2021)
Fusarium sporotrichioides	Head blight	Karlsson et al. (2021)
Microdochium nivale	Fusarium Head Blight	Karlsson et al. (2021)
Nigrospora oryzae	Seed pathogen	Eken et al. (2016)
Parastagonospora nodorum	Septoria nodorum blotch	Bertazzoni et al. (2021)
Pyrenophora tritici-repentis	Tan spot	Moolhuijzen et al. (2022)
Stemphylium vesicarium	Leaf spot	Farag et al. (2022)
Zymoseptoria tritici	Septoria tritici blotch	Goodwin et al. (2011)
B. *Potentially emerging diseases*		
Nigrospora oryzae	Seed pathogen	Eken et al. (2016)
Stemphylium vesicarium	Leaf spot	Farag et al. (2022)
C. *Candidate biological control agents*		
Alternaria alternata	Beneficial | Antagonist	Zheng et al. (2017)
Alternaria infectoria	Beneficial | Antagonist	Shabana et al. (2010)
Aureobasidium pullulans	Beneficial | Antagonist	Wachowska et al. (2014)
Cladosporium cladosporioides	Beneficial | Antagonist	Zhang et al. (2022)
Cladosporium oxysporum	Beneficial | Antagonist	Tyagi et al. (2023)
Epicoccum nigrum	Beneficial | Antagonist	Ogorek et al. (2011)
Meyerozyma guilliermondii	Beneficial | Antagonist	Kthiri et al. (2021)
Penicillium chrysogenum	Beneficial | Antagonist	Barna et al. (2008)

535

536

537 **References**

538 Karlsson, I., Persson, P., Friberg, H. (2021). Fusarium head blight from a microbiome perspective.
539 *Front. Microbiol*. 12, 628373. doi: 10.3389/fmicb.2021.628373.

540 Xu, X.M., Parry, D.W., Nicholson, P. *et al.* (2005). Predominance and association of pathogenic
541 fungi causing Fusarium ear blightin wheat in four European countries. *Eur. J. Plant Pathol* 112,
542 143–154. doi: 10.1007/s10658-005-2446-7

543 Brown, J. K., Chartrain, L., Lasserre-Zuber, P., Saintenac, C. (2015) Genetics of resistance to
544 *Zymoseptoria tritici* and applications to wheat breeding. *Fungal Genet. Biol*. 79, 33-41. doi:
545 10.1016/j.fgb.2015.04.017.

546 Pereira, D., McDonald, B. A., Croll, D. (2020) The genetic architecture of emerging fungicide
547 resistance in populations of a global wheat pathogen. *Genome Biology and Evolution*, 12, 2231-
548 2244, doi: 10.1093/gbe/evaa203

549 Justesen, A.F., Corsi, B., Ficke, A. *et al.* (2021) Hidden in plain sight: a molecular field survey of
550 three wheat leaf blotch fungal diseases in North-Western Europe shows co-infection is
551 widespread. *Eur. J. Plant Pathol.* 160, 949–962. doi: 10.1007/s10658-021-02298-5

552 Jørgensen, L.N., Matzen, N., Heick, T.M. *et al.* (2018). Decreasing azole sensitivity of *Z. tritici* in
553 Europe contributes to reduced and varying field efficacy. *J. Plant Dis. Prot.* 128, 287-301. doi:
554 10.1007/s41348-020-00372-4

555 Jørgensen, L.N., Matzen, N., Heick, T.M., O'Driscoll, A., Clark, B., Waite, K., Blake, J., Glazek, M.,
556 Maumene, C., Couleaud, G., Rodemann, B., Weigand, S., Bataille, C. R. B., Hellin, P., Kildea, S.
557 and Stammler, G. (2022) Shifting sensitivity of septoria tritici blotch compromises field
558 performance and yield of main fungicides in Europe. *Front. Plant Sci*. 13:1060428. doi:
559 10.3389/fpls.2022.1060428.

560 Singh, r. V., Hodson, D. P., Huerta-Espino, J., Jin, Y., Bhavani, S., Njau, P., Herrera-Foessel, S.,
561 Singh, P. K., Singh, S., Govindan, V. (2011). *Annu. Rev. of Phytopathol*. 49, 465-481. doi:
562 10.1146/annurev-phyto-072910-095423

563 Patpour, M., Hovmøller, M.S., Rodriguez-Algaba, J., Randazzo, B., Villegas, D., Shamanin, V.P.,
564 Berlin, A., Flath, K., Czembor, P., Hanzalova, A., Sliková, S., Skolotneva, E.S., Jin, Y., Szabo, L.,
565 Meyer, K.J.G., Valade, R., Thach, T., Hansen, J.G. and Justesen, A.F. (2022) Wheat stem rust

566 back in europe: diversity, prevalence and impact on host resistance. *Front. Plant Sci*. 13:882440.
567 doi: 10.3389/fpls.2022.882440

568 Menardo, F., Praz, C., Wyder, S. *et al.* (2016) Hybridization of powdery mildew strains gives rise to
569 pathogens on novel agricultural crop species. *Nat. Genet.* **48**, 201-205. doi: 10.1038/ng.3485.

570 Huang, S., Pang, F. (2017). Biocontrol agents for controlling wheat rust. In: Periyannan, S. (eds)
571 Wheat rust diseases. *Methods Mol. Biol*. 1659. Humana Press, New York, NY. doi: 10.1007/978-
572 1-4939-7249-4-24

573 Yue, H.M., Wang, M., Gong, W-F., Zhang, L-Q. (2018) The screening and identification of the
574 biological control fungi *Chaetomium* spp. against wheat common root rot, *FEMS Microbiol.*
575 *Letters.* 365, fny242. doi: 10.1093/femsle/fny242

576 Rojas, E.C:, Jensen, B:, Jørgensen, H.J.L. Latz, M.A.C., Esteban, P., Ding, Y., Collinge, D.B. (2020).
577 Selection of fungal endophytes with biocontrol potential against Fusarium head blight in wheat.
578 *Biological Control*, 144, 104222. doi: 10.1016/j.biocontrol.2020.104222.

579 Fagundes, W. C.; Haueisen, J., Stukenbrock, E.H. (2020). Dissecting the biology of the fungal wheat
580 pathogen *Zymoseptoria tritici*: a laboratory workflow. *Curr. Protocols in Microbiol*. 59, e128. doi:
581 10.1002/cpmc.128

582 White, T.J. (1990) Amplification and direct sequencing of fungal ribosomal RNA genes for
583 phylogenetics. In: PCR Protocols, a Guide to Methods and Applications, 315-322.
584 doi:10.1016/B978-0-12-372180-8.50042-1

585 de Biazio, G.R., Leite, G.G., Tessmann, D.J., Barbosa-Tessmann, I.P. (2008) A new PCR approach
586 for the identification of *Fusarium graminearum*. *Braz. J. Microbiol*. 39, 554-60. doi:
587 10.1590/S1517-838220080003000028.

588 Astrid Bauer, R.S., Seigner, L. (2015). Detection, identification and quantification of *Fusarium*
589 *graminearum* and *Fusarium culmorum* in wheat kernels by PCR techniques. *Jour. Plant Pathol.*
590 *Microbiol*. 6, 7. doi: 10.4172/2157-7471.1000287

591 Schindelin, J., Arganda-Carreras, I., Frise, E. et al. (2012) Fiji: an open-source platform for
592 biological-image analysis. *Nat Methods* 9, 676–682. doi: 10.1038/nmeth.2019

593 R Core Team (2021). R: A language and environment for statistical computing. R Foundation for
594 Statistical Computing, Vienna, Austria. URL https://www.R-project.org/

595 DeMers M. (2022) *Alternaria alternata* as endophyte and pathogen. *Microbiol.* 168, 001153. doi:
596 10.1099/mic.0.001153

597 Liu, L., Zhao, K., Zhao, Y., Zhang, Y., Fu, Q., Shiwen, H. (2021) *Nigrospora oryzae* causing panicle
598 branch rot disease on *Oryza sativa* (rice). *Plant Dis.* 105, doi: 10.1094/PDIS-11-20-2423-PDN.

599 Mohamed, M.E. (2022) Detection and molecular diagnosis of Stemphylium vesicarium isolated from
600 wheat spikes. *Egypt. Jour. Phytopath*. 50, 63-68. doi: 10.21608/ejp.2022.166572.1072.

601 Fones, H.N., Soanes, D., Gurr, S.J. (2023) Epiphytic proliferation of *Zymoseptoria tritici* isolates on
602 resistant wheat leaves. Fung. Genet. Biol. 168, 103822. doi: 10.1016/j.fgb.2023.103822.

603 Seybold, H., Demetrowitsch, T.J., Hassani, M.A. *et al.* (2020) A fungal pathogen induces systemic
604 susceptibility and systemic shifts in wheat metabolome and microbiome composition. *Nat.*
605 *Commun.* 11, 1910. doi: 10.1038/s41467-020-15633-x

606 Köhl, J., Kolnaar, R. and Ravensberg, W.J. (2019) Mode of action of microbial biological control
607 agents against plant diseases: relevance beyond efficacy. *Front. Plant Sci.* 10:845. doi:
608 10.3389/fpls.2019.00845

609 Zheng, L., Zhao, J., Liang, X., Zhan, G., Jiang, S. and Kang, Z. (2017) Identification of a novel
610 *Alternaria alternata* strain able to hyperparasitize *Puccinia striiformis* f. sp. *tritici*, the causal
611 agent of wheat stripe rust. *Front. Microbiol*. 8:71. doi: 10.3389/fmicb.2017.00071

612 Zhang, H., He, M., Fan, X., Dai, L., Zhang, S., Hu, Z., Wang, N. (2022) Isolation, identification and
613 hyperparasitism of a novel *Cladosporium cladosporioides* isolate hyperparasitic to *Puccinia*
614 *striiformis* f. sp. *tritici*, the wheat stripe rust pathogen. *Biology* 11, 892. doi:
615 10.3390/biology11060892.

616 El-Sharkawy, H.H.A., Rashad, Y.M., Elazab, N.T. (2023) Biocontrol potential of the endophytic
617 *Epicoccum nigrum* HE20 against stripe rust of wheat. *Pestic. Biochem. Physiol*. 194, 05517. doi:
618 10.1016/j.pestbp.2023.105517

619 Wachowska, U., Głowacka, K., Mikołajczyk, W. et al. (2016) Biofilm of *Aureobasidium pullulans*
620 var. *pullulans* on winter wheat kernels and its effect on other microorganisms. *Microbiol.* 85, 523–
621 530. doi: 10.1134/S0026261716050192

622 Kthiri, Z., Jabeur, M. B., Chairi, F., López-Cristoffanini, C., López-Carbonell, M., Serret, M. D.,
623 Araus, J. L., Karmous, C., Hamada, W. (2021) Exploring the potential of *Meyerozyma*

guilliermondii on physiological performances and defense response against Fusarium crown rot on durum wheat. *Pathogens* 10, 52. doi: 10.3390/pathogens10010052

Ma, H., Duan, X., Xu, W., Ma, G., Ma, W., Qi, H. (2022) Root rot of *Angelica sinensis* caused by *Clonostachys rosea* and *Fusarium acuminatum* in China. *Plant Dis.* 106:8, 2264. doi: 10.1094/PDIS-12-21-2665-PDN

Hexing Qi, Xiaoming Duan, Wenhua Xu, Yuantao Zhou, Haixia Ma, Weili Ma, and Guihua Ma (2022) First report disease of *Clonostachys rosea* causing root rot on *Astragalus membranaceus* in China. *Plant Dis.* 106, 6. doi: 10.1094/PDIS-07-21-1511-PDN

Diaz, R., Chavez, E.C., Delgado Ortiz, J.C., Velazquez, J.J., Roque, A., Ochoa, Y.M. (2022) First report of *Clonostachys rosea* causing root rot on garlic in Mexico. *Plant Dis*. 106:11 doi: 10.1094/PDIS-12-21-2658-PDN.

Afshari, N., Hemmati, R. (2017) First report of the occurrence and pathogenicity of *Clonostachys rosea* on faba bean. *Australasian Plant Pathol*. 46, 231-234 doi:10.1007/s13313-017-0482-3

Coyotl-Pérez, W.A., Romero-Arenas, O., Mosso-González, C., Pacheco-Hernández, Y., Rivera-Tapia J.A., Villa-Ruano, N. (2022) First report of *Clonostachys rosea* associated with avocado fruit rot in Puebla, Mexico. *Rev. Mex. Phytopathol* 40, 298-307. doi: 10.18781/r.mex.fit.2203-5

Zhang, Y., Yu, H., Hu, M., Wu, J., Zhang, C. (2022) Fungal pathogens associated with strawberry crown rot disease in china. *J. Fungi* 8, 1161. doi:10.3390/jof8111161

Haque, M.E. and Parvin, M.S. (2020) First report of *Clonostachys rosea* causing root rot of *Beta vulgaris* in North Dakota, USA. *New Disease Reports*, 42, 21-21. doi: 10.5197/j.2044-0588.2020.042.021.

Farhaoui, A., Tahiri, A., Radouane, N., Khadiri, M., Amiri, S., El Alami, N. et al. (2023) First report of *Clonostachys rosea* causing sugar beet root rot in Morocco. *New Disease Reports*, 48, e12235. doi: 10.1002/ndr2.12235

Jin, M., Yang, C., Wang, Y., Wei, L. & Osei, R. (2023) Isolation and identification of *Epicoccum nigrum* as the causal agent of brown spot disease in *Solanum tuberosum* in China. *Plant Pathol*. 72, 829-838. doi: 10.1111/ppa.13696.

Blumenstein, K., Bußkamp, J., Langer, G.J., Terhonen, E. (2022) Diplodia tip blight pathogen's virulence empowered through host switch. *Front. Fungal Biol*. 3: 939007. doi: 10.3389/ffunb.2022.939007

654 Peeters, K.J., Audenaert, K., Höfte, M. (2021) Survival of the fittest: how the rice microbial
655 community forces *Sarocladium oryzae* into pathogenicity. *FEMS Microbiol. Ecol*. 97:fiaa253. doi:
656 10.1093/femsec/fiaa253

657 Schiro, G., Verch, G., Grimm, V., Müller, M.E.H. (2018) Alternaria and Fusarium fungi: differences
658 in distribution and spore deposition in a topographically heterogeneous wheat field. J. Fungi 4:63.
659 doi: 10.3390/jof4020063.

660 Nzabanita, C., Zhang, L., Zhao, H., Wang, Y., Wang, Y., Sun, M., Wang, S., Guo, L. (2022) Fungal
661 endophyte *Epicoccum nigrum* 38L1 inhibits in vitro and in vivo the pathogenic fungus *Fusarium*
662 graminearum. *Biological Control* 174: 397-408. doi: 10.1016/j.biocontrol.2022.105010.

663 Rojas, E.C., Sapkota, R., Jensen, B., Jørgensen, H.J.L., Henriksson, T., Jørgensen, L.N., Nicolaisen,
664 M., Collinge, D.B. (2020) Fusarium head blight modifies fungal endophytic communities during
665 infection of wheat spikes. *Microb. Ecol.* 79:397-408. doi: 10.1007/s00248-019-01426-3

666 Eken, C., Spanbayev, A., Tulegenova Z., Yechshzhanov, T. (2016) First report of *Nigrospora oryzae*
667 on wheat in Kazakhstan. *Plant Dis*. 4:861-861. doi: 10.1094/PDIS-08-15-0915-PDN.

668

669